Fermi National Accelerator Laboratory

FERMILAB-Conf-88/199-E
[E-735]

Quark Gluon Plasma - Overview and Experimental Results from E-735*

Frank Turkot
Fermi National Accelerator Laboratory
P.O. Box 500, Batavia, Illinois 60510

For the FNAL E-735 Collaboration

T. Alexopoulos[6], C. Allen[5], E. W. Anderson[3], H. Areti[2], S. Banerjee[4], P. D. Beery[4], N. N. Biswas[4], A. Bujak[5], D. D. Carmony[5], T. Carter[1], P. Cole[5], Y. Choi[5], R. De Bonte[5], A. Erwin[6], C. Findeisen[6], A. T. Goshaw[1], L. J. Gutay[5], A. S. Hirsch[5], C. Hojvat[2], V. P. Kenney[4], D. Koltick[5], C. S. Lindsey[3], J. M. LoSecco[4], T. McMahon[5], A. P. McManus[4], N. Morgan[5], K. Nelson[6], S. H. Oh[1], J. Piekarz[4], N. T. Porile[5], D. Reeves[2], R. P. Scharenberg[6], B. C. Stringfellow[5], S. R. Stampke[4], M. Thompson[6], F. Turkot[2], W. D. Walker[1], C. H. Wang[3], and D. K. Wesson[1]

[1] Department of Physics, Duke University, Durham, North Carolina 27706
[2] Fermi National Accelerator Laboratory, Batavia, Illinois 60510
[3] Department of Physics, Iowa State University, Ames, Iowa 50011
[4] Department of Physics, University of Notre Dame, Notre Dame, Indiana 46556
[5] Department of Physics and Chemistry, Purdue University, West Lafayette, Indiana 47907
[6] Department of Physics, University of Wisconsin, Madison, Wisconsin 53706

December 14, 1988

*Presented by F. Turkot at the 7th Topical Workshop on Proton-Antiproton Collider Physics, Fermilab, June 20-24, 1988.

Operated by Universities Research Association Inc. under contract with the United States Department of Energy

QUARK GLUON PLASMA - OVERVIEW AND EXPERIMENTAL RESULTS FROM E-735

Frank Turkot

Fermilab, Batavia, Illinois 60510, U.S.A.

For the FNAL E-735 Collaboration

T. Alexopoulos[6], C. Allen[5], E.W. Anderson[3], H. Areti[2], S. Banerjee[4], P.D. Beery[4], N.N. Biswas[4], A. Bujak[5], D.D. Carmony[5], T. Carter[1], P. Cole[5], Y. Choi[5], R. De Bonte[5], A. Erwin[6], C. Findeisen[6], A.T. Goshaw[1], L.J. Gutay[5], A.S. Hirsch[5], C. Hojvat[2], V.P. Kenney[4], D. Koltick[5], C.S. Lindsey[3], J.M. LoSecco[4], T. McMahon[5], A.P. McManus[4], N. Morgan[5], K. Nelson[6], S.H. Oh[1], J. Piekarz[4], N.T. Porile[5], D. Reeves[2], R.P. Scharenberg[6], B.C. Stringfellow[5], S.R. Stampke[4], M. Thompson[6], F. Turkot[2], W.D. Walker[1], C.H. Wang[3], and D.K. Wesson[1]

[1]Department of Physics, Duke University, Durham, North Carolina 27706

[2]Fermi National Accelerator Laboratory, Batavia, Illinois 60510

[3]Department of Physics, Iowa State University, Ames, Iowa 50011

[4]Department of Physics, University of Notre Dame, Notre Dame, Indiana 46556

[5]Department of Physics and Chemistry, Purdue University, West Lafayette, Indiana 47907

[6]Department of Physics, University of Wisconsin, Madison, Wisconsin 53706

ABSTRACT

A brief review of the phenomenology associated with the effort to produce and observe quark-gluon plasma in particle collisions is presented. E-735 has taken data during the 1987 Tevatron-Collider run at $\sqrt{s}=$ 1.8 TeV in pursuit of this goal. Results in the correlation of $< p_t >$ with multiplicity for charged particles and p_t distributions for Λ^0 and $\bar{\Lambda}^0$ are presented.

1. OVERVIEW OF QUARK GLUON PLASMA PHYSICS

There has been an impressive growth in this field - mostly theoretical - over the past eight years; it has intensified since 1986 with the advent of data from experiments at CERN and Brookhaven using relativistic ^{16}O and ^{32}S beams. Perhaps the most useful thing I can do at the outset is to point out the excellent review article by Kajantie and McLerran[1] for theory and the Quark Matter 1987 proceedings[2] for experiment.

1.1 QCD Matter at High Density

In 1975, Collins and Perry[3] suggested that normal nuclear matter of energy density $\epsilon = 0.13\ GeV/fm^3$ would become a plasma of quarks and gluons (QGP) at higher density, somewhere above the density inside of a single nucleon, $\epsilon = 0.42\ GeV/fm^3$. The idea being that when hadrons overlap sufficiently, the color charge of a quark in any particular hadron will be screened by all of the nearby quarks; consequently the local confinement is broken and the colored partons are free to roam about throughout the superdense matter, as in a plasma. The dense overlapping hadron condition can be achieved by compressing the normal nuclear matter or by creating new hadrons to fill the space by raising the temperature. Hence, QCD matter undergoes a deconfining phase transition from normal hadrons to QGP at sufficiently high ϵ. The conjectured phase diagram of QCD matter is shown in Fig. 1; the abscissa is net baryon density, the ordinate temperature. The region in the QGP phase at low T and high B is the condition which may exist at the center of neutron stars, while the region near B=O and high T is thought to be the condition of the early universal at $t \sim 1 \times 10^{-6} s$.

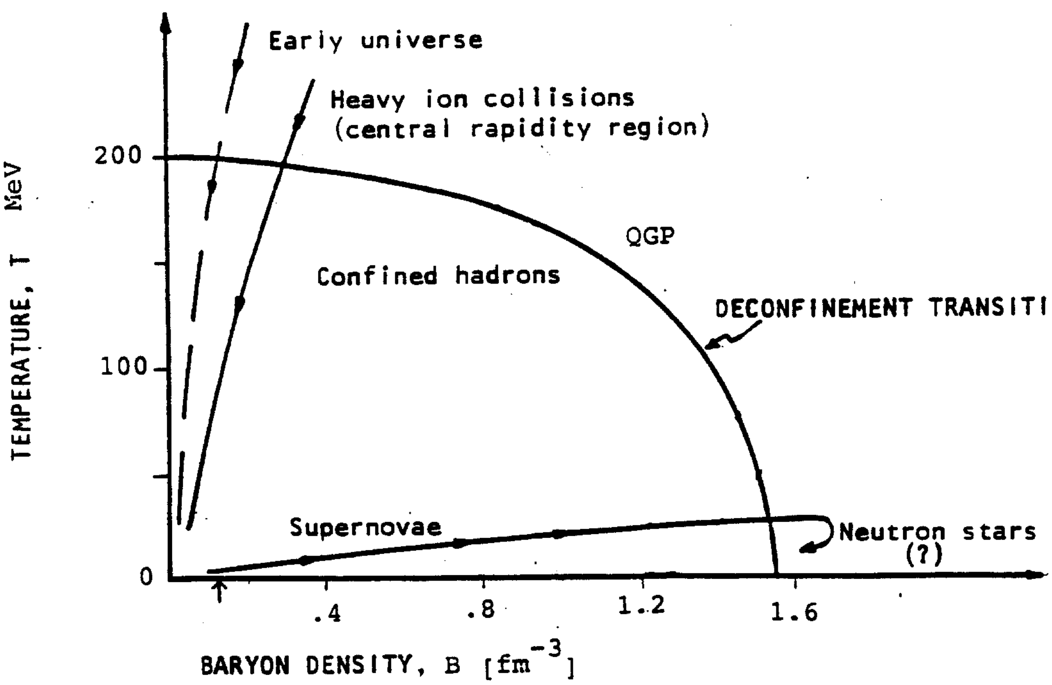

Figure 1: Theoretical phase diagram in the temperature - net baryon density plane.

Soon after Perry and Collins, there arose speculation[4] that sufficient ϵ could be achieved in relativistic nucleus-nucleus collisions to form the QGP phase. In 1982 the observation by the UA1 and UA2[5] experiments at CERN of $\bar{p}p$ collisions with 60 GeV of isotropic transverse energy, E_t , led Bjorken[6] to suggest that QGP could be made in $\bar{p}p$ collisions at $\sqrt{s} = 540$ GeV as well.

Compared to the situation in neutron stars or the early universe, the QGP formed in particle collisions is very short-lived, it decays in $\sim 5 \times 10^{-23} s$ back to hadrons, leptons, and photons. The real challenge of the field has been to understand what experimental observables will: (a) give clear evidence of the QGP existence in the collision and (b) allow one to study the properties and behaviour of QCD matter in the region of the phase transition. There is an ongoing program to calculate the *static* properties of QCD matter from first principles using the method of Monte Carlo lattice simulation[7]. Figure 2 shows the results for the equation-of-state in the transition region for the case of B $\simeq$ 0; it shows a first-order phase transition that enters the mixed-phase at $\epsilon = \epsilon_H = 1.5\ GeV/fm^3$ and becomes pure QGP at $\epsilon = \epsilon_Q = 4.0\ GeV/fm^3$.

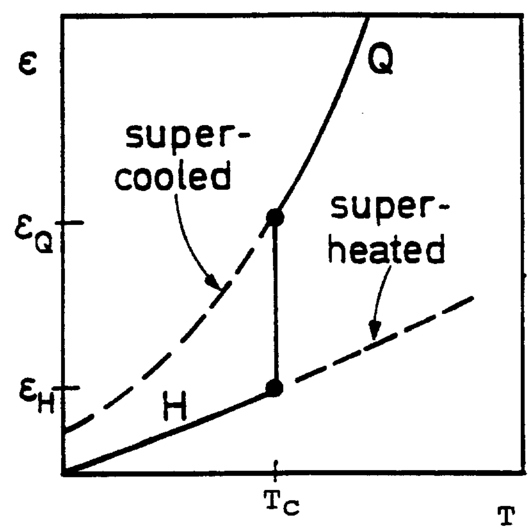

Figure 2: Equation of state for QCD matter with B=0, first-order phase transition.

The latent heat is $\epsilon_Q - \epsilon_H = 2.5\ GeV/fm^3$ and the critical temperature, T_c is 200 MeV (the actual values for ϵ_H and ϵ_Q are quite uncertain, perhaps as large as a factor of 2). For $T >> T_c$, asymptotic freedom implies that the QGP becomes a pure Stephan-Boltzmann gas of massless quarks and gluons. The calculations are difficult and there remain some important open questions. The Debye screening length for the color fields in the QGP, which is relevant to the suppression of J/ψ production in collisions, has also been calculated on the lattice.

1.2 Space-Time Evolution in Particle Collisions

In order to predict the final state observables (e.g., the number and energy distribution of photons) which could signal the production of QGP in the collisions one must know in some detail the transient behaviour of the system in the $\sim 10^{-22}$s period following the initial interaction. The description of the evolution in space-time is visualized with the aid of the Minkowski diagram of Fig. 3, where Z is the collision axis.

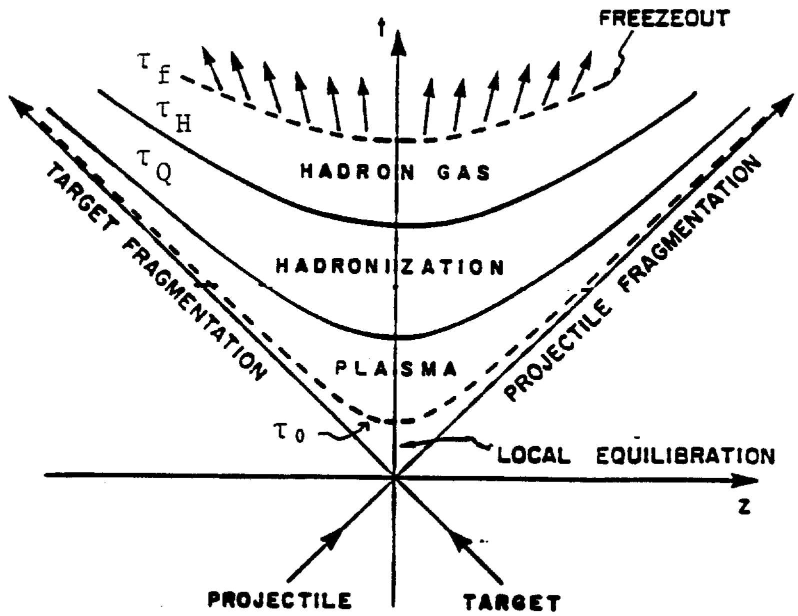

Figure 3: Longitudinal evolution of an ultrarelativistic collision.

Bjorken[8] has given a hydrodynamic model of the evolution which incorporates the observed fact of a flat rapidity (y) distribution of particle production in the central region for nucleon-nucleon collisions, this model is often referred to as "scaling" or "boost invariant" hydrodynamics. As seen in Fig. 3, one can distinguish five stages in the evolution, each of which is bounded by "proper-time" hyperbolas. In this model, it is assumed that at an initial proper-time $\tau_0(\simeq 1\ fm/c)$ there exists a QGP in local termal equilibrium with uniform energy density ϵ_0, longitudinal velocity Z/t, and zero transverse velocity. It is allowed to expand as a perfect fluid, at τ_Q it has cooled to T_c and enters the mixed-phase of QGP and hadron "gas"; the mixed phase continues to expand at constant $T = T_c$ and pressure until τ_H where it becomes a pure hadron gas; the hadron gas continues to expand and cool until τ_f ("freeze-out") where it turns into freely streaming hadrons. The actual time evolution is thus determined by the initial conditions and the equation-of-state of the QCD matter; for U-U collisions he estimates $\tau_f \sim 10 - 20\ fm/c$. This model is less applicable to the case of $\bar{p}p$ collisions due to the much smaller initial transverse dimension of the interaction volume.

Based on this model, Bjorken derives a formula (expected to be a lower limit) relating ϵ_0 to the rapidity density of hadrons in the *final* state as follows:

$$\epsilon_0 = \frac{< m_\tau >}{c\tau_0 A_t} \frac{dN}{dy} \quad , \tag{1}$$

where $m_t = \sqrt{p_t^2 + m^2}$ and A_τ is the transverse area of the initial interaction volume. If we evaluate this for $\bar{p}p$ at $\sqrt{s} = 1.8$ TeV (using $< m_t > = 0.5\ GeV/c^2$, $c\tau_0 = 1\ fm$, and $A_t = \pi R^2$ with $R = 1.0\ fm$ as indicated from the inelastic cross-section) we obtain

$$\epsilon_0 = 0.24 \frac{dN_c}{dy}\ GeV/fm^3 \quad , \tag{2}$$

which gives for the average collision, $\frac{dN_c}{dy} = 4$, a value $0.96\ GeV/fm^3 (= 0.6\epsilon_H)$; according to this estimate no QGP is produced in the *average* $\bar{p}p$ collision at this energy.

1.3 QGP Signatures

We turn now to the experimental observables that could signal the existence of QGP in particle collisions and yield information on its properties.

1.3.1 Dependence of $< p_t >$ on dN/dy and particle mass. In 1982 the UA1 experiment[9] showed a dramatic increase (~35%) of $< p_t >$ with dN_c/dy for centrally produced ($|y| < 2.5$) charged particles (see Fig. 7) in $\bar{p}p$ at $\sqrt{s} = 540\ GeV$; the rate of increase slows for $dN_c/dy > 7$ and the data suggest a plateau for $10 < dN_c/dy < 17$. Van Hove[10] argued that this behaviour was a possible signature of the phase transition, i.e., it has the same qualitative fixtures of the equation-of-state of Fig. 2, where $< p_t >$ plays the role of T and dN_c/dy the role of ϵ_0 vs. Eq. 2. He also pointed out that the p_t spectrum reflects the combined effects of T (at freeze-out time) *and* the transverse expansion of the matter and hence the plateau that is seen in ϵ via T for a first order phase transition could develop a slope-in $< p_t >$ vs. dN_c/dy. Since then, there have been a number of calculations[11] which treat the space-time evolution in fair detail (QGP droplet formation and shock waves during the mixed-phase) and make quantitative predictions for $< p_t >$. Figure 4 is an example[12] which gives $< p_t >$ for π, K, and p separately; the faster increase of $< p_t >$ with mass is due to the common transverse velocity imparted by the expansion. The second curve for π's shows the behaviour if there is no phase transition. Note that the "plateau," corresponding to the mixed-phase at $T = T_c$, has a finite slope. The second rise for $\epsilon > \epsilon_Q$ is a result of increasing the initial temperature and the resulting transverse flow, its appearance is enhanced by the $ln(A^{-1}dN/dy)$ plot.

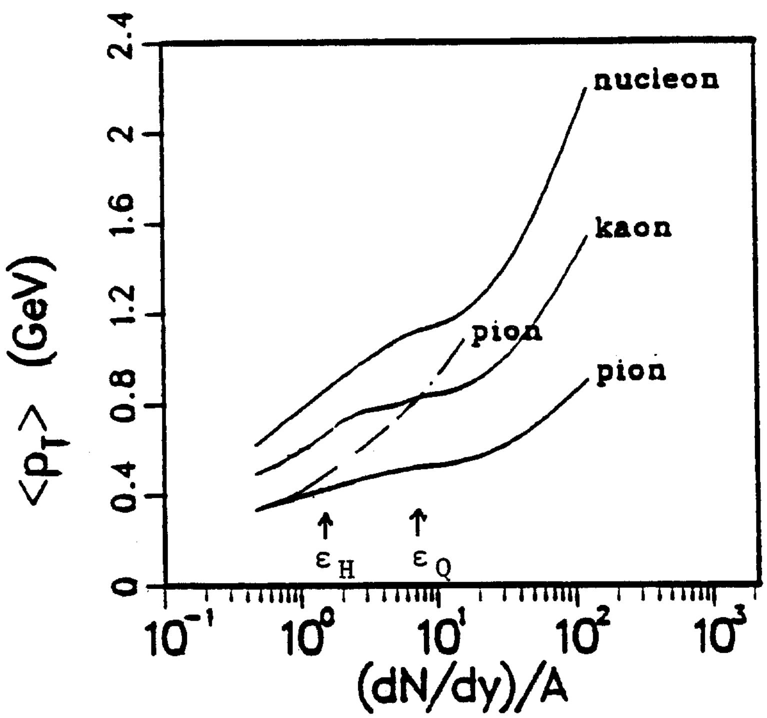

Figure 4: Hydrodynamic model of U-U collision; the second pion curve (broken) is without phase transition.

The above models for nucleus-nucleus collisions indicate a scaling law like

$$< p_t > = F\left(\frac{1}{A}\frac{dN}{dy}\right) = F(x) \quad , \tag{3}$$

which makes it difficult to vary x at a given beam energy (GeV/nucleon) by varying A, since $dN/dy \ \alpha \ A$ for average central collisions. The recent CERN experiments[13] using ^{32}S beams of 200 GeV/c nucleon have reached to $x \simeq 10$; in contrast E-735 has measured $< p_t >$ for dN/dy as large as 30.

1.3.2 Enhancement of K/π, Y/p. The enhancement of strangeness as a signal for QGP production in nucleus-nucleus collisions has been a controversial subject; it was originally thought to be a good indicator[14]. Subsequent treatments[15] show that a quantitative prediction depends strongly on the specific space-time evolution of the QCD matter, in particular the degree of chemical equilibrium achieved during the hadronization stage. The recommendation is to measure several ratios as a function of dN/dy.

1.3.3 Direct photons. Photons have an advantage over hadron signals in that they can come directly from the QGP stage of Fig. 3. Estimates of a γ/π ratio as high as 20% have been made[16]. As with other signals the production mechanisms must be convoluted with the space-time evolution of the QCD matter in order to predict the observable photon spectra. In principle, the photon spectrum in the energy range 0 - 3 GeV can be used to measure the initial high temperature of the QGP phase. A measurement of γ/π as a function of p_t for both low and high values of dN/dy (or E_t) is clearly of interest.

1.3.4 Dileptons. In the QGP phase dileptons are produced by $q+\bar{q} \rightarrow \ell^+ + \ell^-$ and in the hadron phase by $\pi^+ + \pi^- \rightarrow \ell^+ + \ell^-$. There is a correlation between regions of the dilepton mass spectrum and stages during the space-time evaluation[17] as follows: (a) $1 < M < 3$ GeV. The delepton rate in this region is sensitive to the initial temperature of the QGP phase and proportional to $(dN/dy)^2$. Due to the early time of emission transverse flow effects have little influence on the thermal-like shape of the spectrum, (b) $0 < M < 1$ GeV. This region is dominated by $\pi^+\pi^-$ annihilation in the mixed phase and beyond; the spectrum shape is characterized by the ρ peak at 770 MeV. The p_t dependence of the ρ peak is thought to be a good measure of transverse flow that develops during the mixed and hadron phases.

1.3.5 Resonance melting, J/ψ suppression. In 1986, Matsui and Satz[18] predicted that the suppression of J/ψ production in nucleus-nucleus collisions would provide an "unambiguous" signature for QGP formation. They argued that a $c\bar{c}$

bound state will be dissolved by the plasma if the physical size of the state is comparable to the Debye colour screening length of the plasma; this condition is expected to prevail for $T/T_c \geq 1.2$. The NA38 experiment[19] has reported a 40-50% reduction in the ratio of J/ψ to continuum when comparing events at low E_t vs high E_t in both ^{16}O-U and ^{32}S-U collisions at 200 GeV/nucleon. Since the original prediction, alternative explanations of suppression, not invoking QGP, have been made; in addition FNAL experiment E-537 has reported[20] the suppression of J/ψ production in $\pi^- W$ collisions at 125 GeV/c.

1.3.6 Pion interferometry. The correlation function of like-sign pion pairs in momentum space is an observable which can in principle yield the space-time structure of the matter in the vicinity of freeze-out. Correlation analyses can be parameterized in a variety of ways; due to the possible correlations that exist in these collisions between coordinate and momentum space, care must be taken in the interpretation of geometrical parameters deduced in a given analysis[21]. As an example, the NA35 experiment at CERN has found[22] a surprisingly large transverse dimension (8 fm) for the central region in ^{16}O+Au. The hope is that pion interferometry will be a useful tool in defining explicit dynamical models of the collisions.

2. THE E-735 DETECTOR

The E-735 detector was designed to study low p_t (0.1 - 3 GeV/c) particle production in the central region ($|\eta| < 3$, η being pseudorapidity) of $\bar{p}p$ collisions at $\sqrt{s} \simeq 1.8$ TeV. We had in mind the first three QGP signatures discussed in Section 1.3 together with auxiliary information from $\pi - \pi$ interferometry. The idea was to study production over a broad range of $dN_c/d\eta$ from 1/2 to ~ 8 times $< dN_c/d\eta >$.

As seen in Fig. 5 the actual detector consists of three major parts: (a) a symmetric central tracking system covering $|\eta| < 3.25$ consisting of scintillation counters and drift chambers, (b) a symmetric set of scintillation counters close to the beam, $3 < |\eta| < 4.5$, for selecting minimum bias beam-beam events and measuring flight time, and (c) a magnetic spectrometer arm with time-of-flight at roughly 90^0 ($-0.36 < \eta < 1.0$, referenced to proton direction) that samples about 1% of the $\eta - \phi$ space covered by the central-tracking system. The central-tracking is provided by a 2m - long cylindrical JADE - type chamber (CTC) utilizing a foam-carbon fiber shell; both ends of the CTC are closed with endcap chambers having radial wires.

The central hodoscope consists of 98 counters in a cylinder outside of the CTC and two 3-ring endcaps with 72 counters each, summing to 240 elements in total.

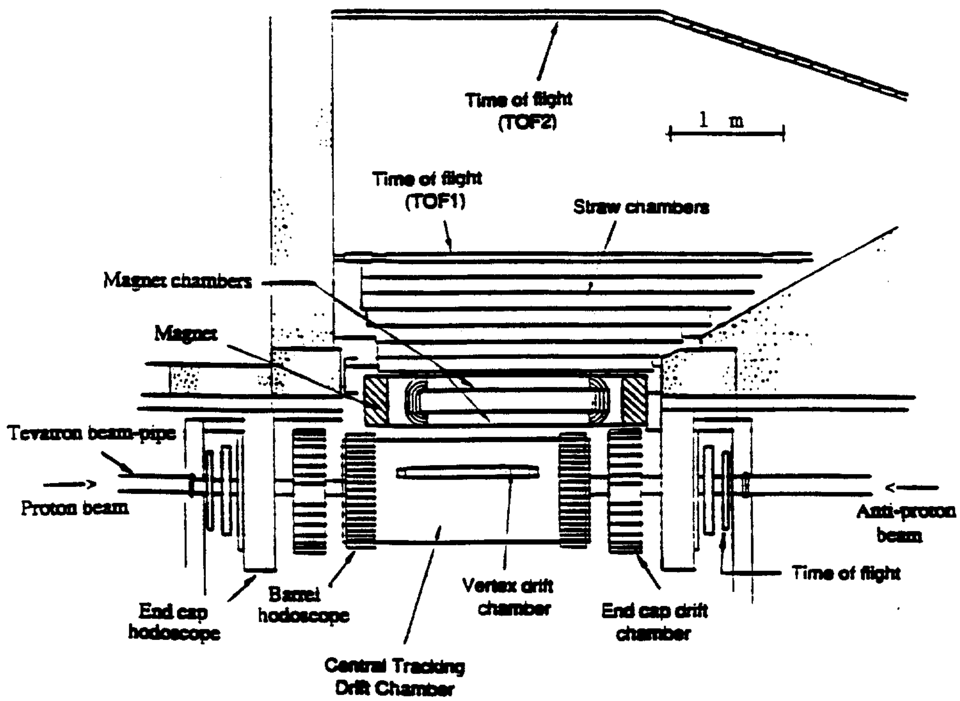

Figure 5: Plan view of E-735 experimental apparatus.

Charged particles which enter the spectrometer arm are tracked by four sets of drift chambers and their flight times recorded in two banks of scintillation counters, one at 2m (TOF 1) from the beamline and one at 4m (TOF 2). The range cutoff for π's to reach TOF 1 is ~100 MeV/c. With the magnet set for a 50 MeV/c transverse kick, the spectrometer yields a σ_p/p ~7% at 1 GeV/c. The TOF system[23] is capable of kaon identification up to 1.5 GeV/c and nucleon identification to 1.9 GeV/c.

This detector resides at the C0 interaction region of the Collider, which has a $\beta^* = 75$m for the normal lattice. The peak luminosity during the 1987 data run was $\sim 1 \times 10^{27}$ $(cm^2 \cdot s)^{-1}$, resulting in a minimum bias trigger rate of 50 Hz. A fast-trigger processor which reads total multiplicity, N_h, in the central hodoscope preferentially selects large N_h in order to match the data acquisition capability of 10 Hz.

3. RESULTS FROM THE 1987 COLLIDER RUN

The data presented here were taken during the commissioning run of the Tevatron Collider which occurred during the first half of 1987. The configuration of the detector was as described above minus the CTC and half of the endcap chambers. In this 13 - week run, we recorded some 4 million triggers with an integrated luminosity of 1/3 nb^{-1}. The statistics of the event class having at least one good track in the spectrometer are given in Table I.

Table I.

Event Type	No. of Spectrometer Tracks	No. of Events
All Charged	≥ 1	500K
	≥ 2	170K
$\pi\pm$	≥ 1	200K
	≥ 2	80K
$K\pm$	≥ 1	8K
$p\pm$	≥ 1	5K
Λ^0 or $\bar{\Lambda}^0$	≥ 2	0.4K

We show results from the "all charged" and the $\Lambda^o/\bar{\Lambda}^o$ categories in what follows.

3.1 Single Particle p_t Spectra and $< p_t >$ vs Multiplicity.

Our results on charged-particle spectra (without particle identification) were reported[24] previously; for the details of the analysis we refer the reader to that source. The main challenge was to relate the true number of charged tracks, N_c, in the central hodoscope region ($|\eta| < 3.25$) to the number of hits N_h recorded in the counters. This was done through Monte Carlo simulation and checked by using track distributions observed in the spectrometer arm; the value of N_c so determined has an estimated uncertainty of 10%.

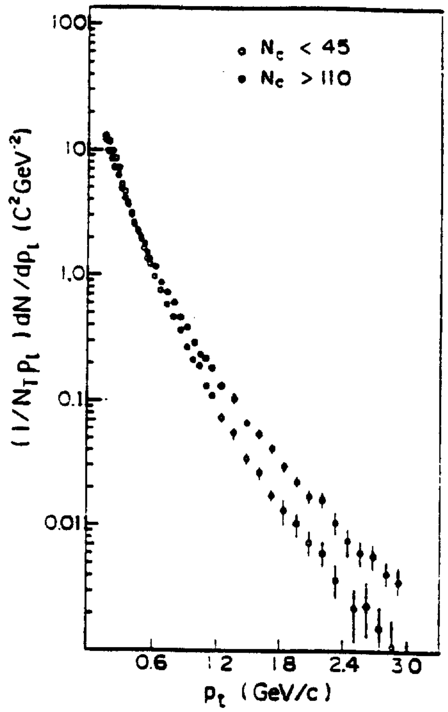

Figure 6: Normalized single-particle p_t distribution for two different multiplicity regions.

In Fig. 6, we see the p_t spectra from 0.15 GeV/c to 3.0 GeV/c for $N_c <$ 45 and $N_c > 110$ (minimum-bias events have $< N_c > \simeq 30$); the flattening of the spectrum with larger N_c as first observed by UA1[9] at $\sqrt{s} = 540$ GeV is evident. In order to calculate $< p_t >$, the contribution from the region below 0.15 GeV/c must be included. Extrapolation of dN/dp_t^2 to $p_t = 0$ was done by fitting the data in the region 0.15 to 0.5 GeV/c with the function exp $(-bp_t)$. Table II lists our value of $< p_t >$ for minimum bias events along with two other values reported at this conference (all extrapolate to $p_t = 0$).

Table II.

Experiment	$\sqrt{s}$ TeV	$p_{t\,min}$ GeV/c	$p_{t\,max}$ GeV/c	$< p_t >_{MB}$ GeV/c
E-735	1.8	0.15	3.0	0.46 ± 0.01
CDF[25]	1.8	0.4	9.0	$0.495 \pm 0.014 \pm 0.02$
UA1[26]	0.9	0.15	9.0	0.447 ± 0.004

We estimate that the region of $< p_t >$ above 3 GeV/c would increase the E-735 average by 2.5%. Taken at face value it appears that $< p_t >_{MB}$ increases by 7% as $\sqrt{s}$ doubles from 0.9 to 1.8 TeV; compared to ISR energy it has risen 32%.

Using this procedure to obtain $< p_t >$, one can compute it for a given small interval of N_c (centered at $\bar{N}_c$), since the central hodoscope covers the region -3.25$< \eta <$3.25 we can use the average particle density variable.

$$\left\langle \frac{dN_c}{d\eta} \right\rangle = \frac{\bar{N}_c}{\Delta\eta} = \frac{\bar{N}_c}{6.5} \qquad (4)$$

In Fig. 7 we show our data for negative particles as a function of this variable; also plotted is the original UA1 data[9] at $\sqrt{s}$= 0.54 TeV and the more recent data[27] at $\sqrt{s} = 0.9$ TeV (the horizontal variable for the UA1 data is really $< dN_c/d\eta >$ averaged over $|\eta| < 2.5$). Our measurement nearly doubles the range of $dN_c/d\eta$ achieved by previous experiments. The general agreement between the three data sets in the common region of $dN_c/d\eta$ is reasonably good; differences might be attributed to the facts that: (a) the two detectors have different acceptance, (b) UA1 p_t spectra go to higher p_t, (c) both experiments have $\sim$ 10% uncertainties in the determination of N_c. Our data indicates that the slope of the curve begins to increase again for $dN_c/d\eta > 20$; a feature expected from the hydrodynamic models with QGP formation (see Fig. 4).

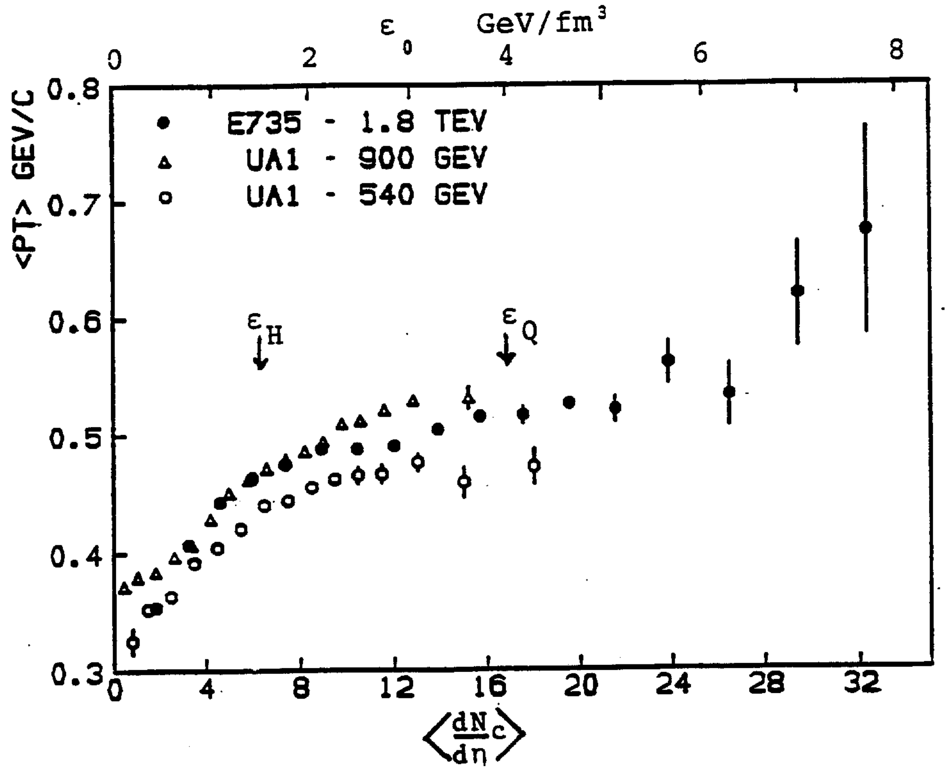

Figure 7: $< p_t >$ vs. $\left\langle \frac{dN_c}{d\eta} \right\rangle$ and initial energy density ϵ_o, negative tracks.

The scale at the top of Fig. 7 is the initial energy density, ϵ_o, as given by Eq. 2; the arrows at ϵ_H, and ϵ_Q mark the region of the mixed phase. Ruuskanen has fitted[12] the E-735 data using a hydrodynamic model and finds a value of T_c = 170 MeV.

As has been the history of QGP signatures, an alternative to the QGP interpretation of the features of Fig. 7 has been made. Jacob[28] proposed that there is a substantial cross-section for low - x QCD minijets arising from gluon-gluon scattering at these energies. A simple two-component model[29] with 12% of minijets, whose $< p_t > = 500$ MeV/c, is able to fit the UA1 data at $\sqrt{s} = 540$ GeV. Wang and Hwa[30] make a more ambitious model which attempts to fit both the $\sqrt{s}$ dependence and the second rise following the plateau.

3.2 Λ^o and $\bar{\Lambda}^o$ Production.

Lambdas produced with $p_t \sim 3$ GeV/c, which head for the spectrometer aperture (see Fig. 5), have a 20% chance that the $p\pi^-$ decay products will tranverse the full spectrometer and be identified. Fig. 8 shows the invariant mass plots for $p\pi^-$ and $\bar{p}\pi^+$ pairs; the shape of the background is obtained by making mass combinations of protons and pions from different events. The fits shown in the figure yield a total of 410 $\Lambda^0 + \bar{\Lambda}^0$ events and the ratio of Λ^0 to $\bar{\Lambda}^0$ of 1.15 ± 0.15. The decay length distribution measured for these events is consistent with $c\tau = 7.9$ cm of Λ^0's.

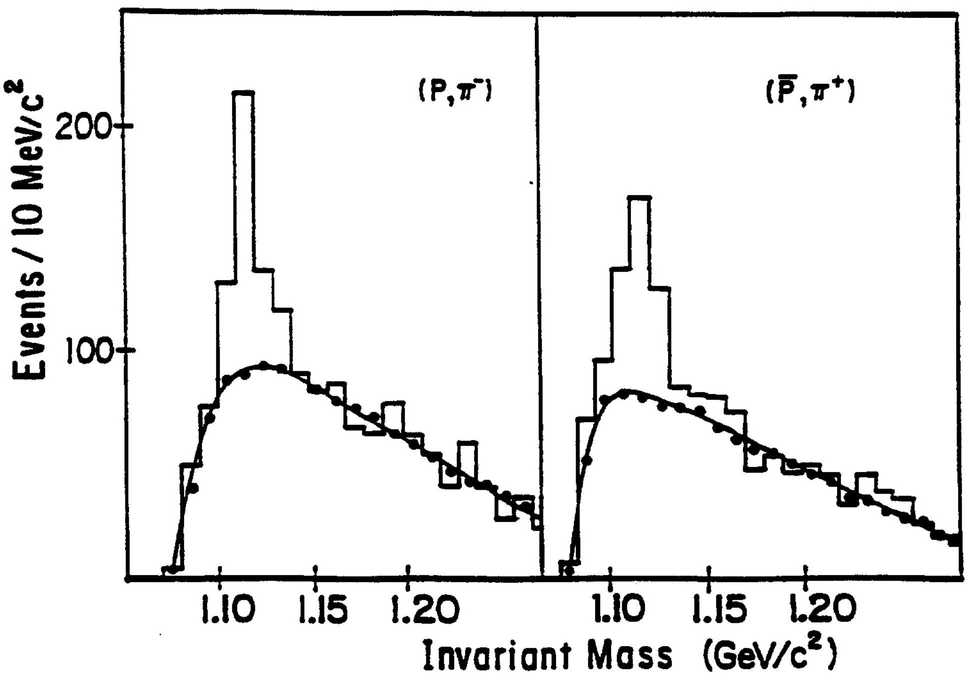

Figure 8: Invariant mass plots for (π^-, p) and $(\pi^+, \bar{p})$.

In Fig. 9(a) we give the p_t distributions for Λ^o, $\bar{\Lambda}^0$, and the sum. Assuming that the exponential curve holds for all p_t, we obtain

$$\langle p_t \rangle_{MB} = 0.80 \pm 0.06 \;\; \text{GeV/c}.$$

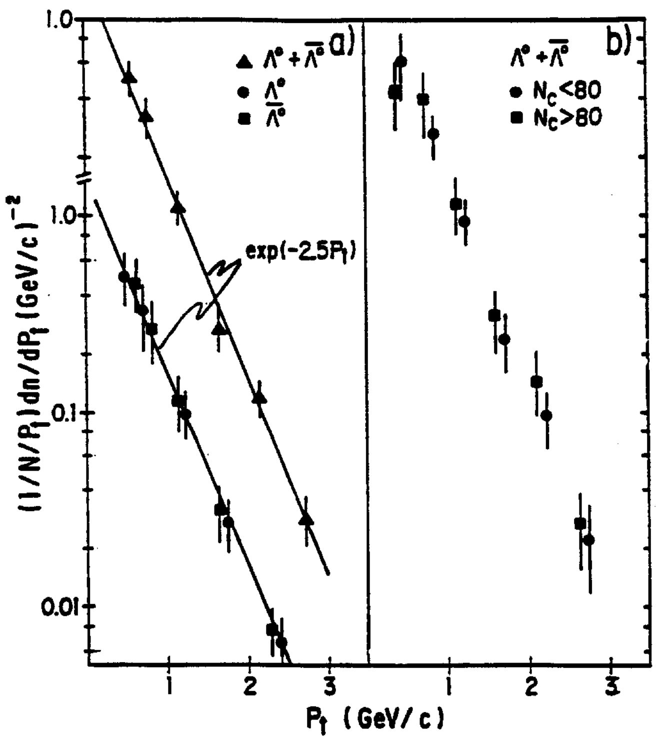

Figure 9: a) p_t distribution of Λ^0, $\bar{\Lambda}^o$, and $\Lambda^o + \bar{\Lambda}^o$.
b) p_t distribution of $\Lambda^0 + \bar{\Lambda}^o$ for two multiplicity regions.

In Fig. 9(b) we examine the dependence of $< p_t >$ on N_c by plotting separately those events with $N_c < 80$ and those with $N_c > 80$; the fitted $< p_t >$ for the latter curve is 11% higher but with marginal statistical significance. Figure 10 exhibits the $\sqrt{s}$ behaviour of $< p_t >_{MB}$ for both $\Lambda^0/\bar{\Lambda}^0$ [31] and "all charged"[32] for ISR energies and above. We note that the fractional increase of $< p_t >$ over this range of $\sqrt{s}$ for $\Lambda^0/\bar{\Lambda}^0$ is approximately twice that of all charged, viz. 60% vs. 32%. Utilizing the data on all charged tracks described in Section 3.1 above, we arrive at an abundance of $\Lambda^0/\bar{\Lambda}^0$ of 3.0 ± 0.3 (statistical) $\pm$ 0.5 (systematic) %, which is about 2.5 larger than that measured[31] at ISR energy.

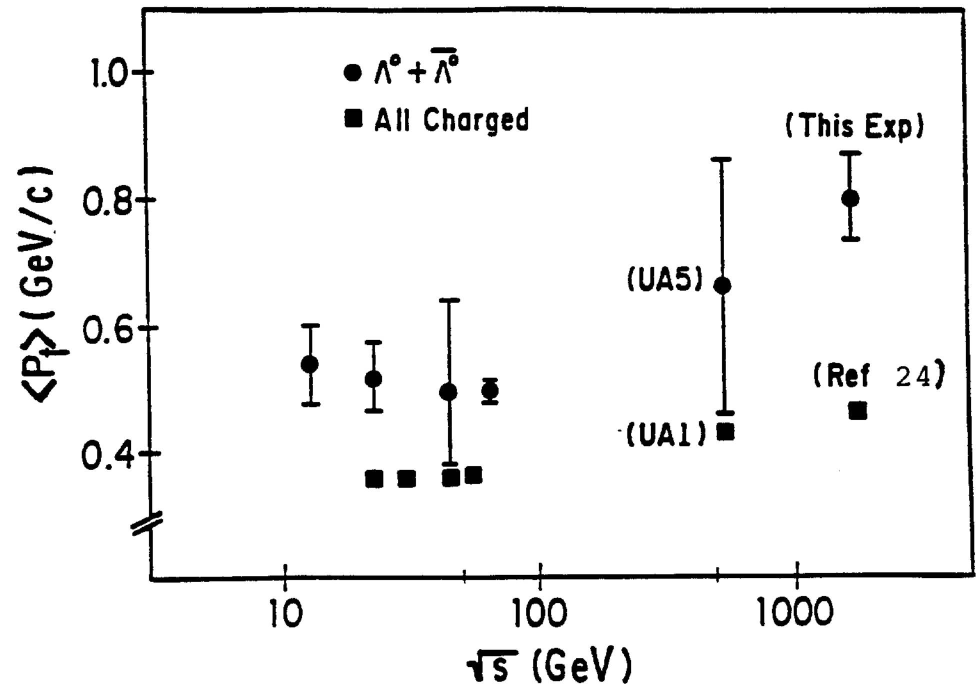

Figure 10: The $< p_t >$ of Λ^0s and of all charged particles as a function of center-of-mass energy.

4. CONCLUSION

There appears to be little doubt that high density QCD matter has been produced in particle collision experiments in the last two years. The ^{32}S + Au experiments at CERN have reached $\epsilon_o \sim 3$ GeV$/_{fm^3}$ by studying average central collisions, and E-735 at Fermilab has reached $\epsilon_o \sim 7$ GeV$/_{fm^3}$ by studying rare events in $\bar{p}p$ where $dN_c/d\eta$ is 7 times the average. There are at least two experimental results which can be explained by the formation of QGP in these collisions. One is the correlation of $< p_t >$ vs. dN_c/dy, first seen in $\bar{p}p$ by UA1 at $\sqrt{s} = 0.54$ TeV as a 35% rise followed by a plateau, and now extended by E-735 at $\sqrt{s} = 1.8$ TeV to show a second rise following the plateau. The second result, which was actually predicted before the measurement, is the suppression of J/ψ production as a function of E_t seen by NA38 in ^{16}O + U and ^{32}S + U collisions at 200 GeV/nucleon. However, plausible explanations have been advanced for both results which do not require the formation of QGP. In the case of $< p_t >$, the models utilize semi-hard

QCD minijets, which in any case should be taken into account. For the J/ψ, the calculations invoke a dense hadron gas and other nucleus effects.

The ambiguity that exists in this field is a consequence of the complexity of the collision process itself and the resultant inability to calculate anything from first principles (some of which are still unknown). Further development of the theory will require close guidance from experiment, and barring some spectacular, unexpected phenomenon, a systematic experimental program to explore all of the observables listed in Section 1.3 is in store.

Data from the 1987 Collider run of E-735 on the p_t spectra of $\pi^{\pm}$, $K^{\pm}$, and $P^{\pm}$ (see Table I) for $dN_c/d\eta$ in the range 2 to 15 will provide a way to look for collective flow effects in $\bar{p}p$ collisions. Particle ratios in this same regime will be forthcoming also. A second Collider run with the full detector is now underway and should yield 10 - 30 times the data sample of the 1987 run, permitting a reach to still higher values of $dN_c/d\eta$.

Acknowledgements

I would like to thank my colleagues in E-735 who produced these results and acknowledge useful disscussions with S.R. Stampke and L. Mc Lerran.

References

1. K. Kajantie and L. Mc Lerran, Ann. Rev. Nucl. Part. Sci. 37, 293 (1987).
2. Proceedings of "Quark Matter 1987", Nordkirchen, W. Germany, Z. Phys. C38 (1988).
3. J.C. Collins and M.J. Perry, Phys. Rev. Lett. 34, 1353 (1975).
4. D.K. Scott, in *Proceedings of the International School of Nuclear Physics, edited by* D. Wilkinson, Prog. in Part. and Nuc. Phy., 4, 5 (1979).
5. UA2 Collaboration, M. Banner *et al.*, Phys. Lett. 118B, 203 (1982).
6. J. Bjorken, *Fermilab Preprint*, Fermilab - Pub - 82/59 - Thy (1982).
7. *For a recent review see* F. Karsch, Z. Phys. C38, 147 (1988).
8. J. Bjorken, Phys. Rev. D 27, 140 (1983).
9. UA1 Collaboration, G. Arnison *et al.*, Phys. Lett. 118B, 167 (1982).
10. L. Van Hove, Phys. Lett. 118B, 138 (1982).
11. G. Baym *et al.*, Nuc. Phy. A407, 541 (1983); M. Kataja *et al.*, Phys. Rev. D

34, 2755 (1986); G. Bertsch *et al.,* Phys. Rev. D 37, 1202 (1988).

12. P.V. Ruuskanen, Univ. of Jyväskylä *preprint* 9/1988 (1988).
13. H.J. Specht, *in the Quark Structure of Matter, edited by* M. Jacob and K. Winter, World Scientific, 417 (1986).
14. J. Rafelski and B. Müller, Phys. Rev. Lett. 48, 1066 (1982).
15. H.W. Barz *et al.,* Nuc. Phy. A484, 661 (1988).
16. F. Halzen and H.C. Liu, Phys. Rev. D 25, 1842 (1982).
17. K. Kajantie *et al.,* Phys. Rev. D 34, 811 (1986).
18. T. Matsui and H. Satz, Phys. Lett 178B, 416 (1986).
19. NA38 Collaboration, A. Bussiere *et al.,* Z. Phys. C38, 117 (1988).
20. S. Katsanevas *et al.,* Phys. Rev. Lett. 60, 2121 (1988).
21. K. Kolehmainen and M. Gyulassy, Phys. Lett. 180B, 203 (1986).
22. NA35 Collaboration, A. Bamberger *et al.,* Phys Lett. 203B, 320 (1988).
23. S. Bannerjee *et al.,* Nim. A269, 121 (1988).
24. T. Alexopoulos *et al.,* Phys. Rev. Lett. 60, 1622 (1988).
25. F. Abe *et al.,* Phys. Rev. Lett. 61, 1819 (1988).
26. J.D. Dowell, *UA1 presentation at this conference.*
27. UA1 Collaboration, G. Piano Mortari, in *Proceedings of the Oregon Meeting, edited by* R.C. Hwa, World Scientific, 615 (1985).
28. M. Jacob, in *Proceedings of the SLAC Topical Conference*, 787 (1983).
29. G. Pancheri and Y. Srivastava, Phys. Lett. 159B, 69 (1985).
30. X. Wang and R.C. Hwa, Univ. of Oregon prepreprint OITS - 387 (1988).
31. A. Sheng *et al.,* Phy. Rev. D 11, 1733 (1975); F. Busser *et al.,* Phys. Lett. 61B, 309 (1976); UA5 Collaboration, Phys. Lett. 115B, 65 (1982).
32. A.M. Rossi *et al.,* Nuc. Phys. B84, 296 (1975); and Ref. 9.